Academic Journal of Science and Technology
ISSN: 2771-3032 | Vol. 20, No. 1, 2026

Finite Element Simulation Analysis of Hydrogen Permeation in 80S Steel

Yimiao Zhang

Mechanical Engineering College, Xi'an Shiyou University, Xi'an, Shaanxi, 710065, China

Abstract: Hydrogen embrittlement poses a serious challenge for high-strength steels (such as 80S steel) when used in hydrogen-containing environments. When hydrogen atoms diffuse into the steel, they can cause local plastic deformation, lattice distortion and even crack propagation, thereby significantly reducing the material's toughness and load-bearing capacity. Research indicates that hydrogen embrittlement is one of the primary safety hazards associated with the use of high-strength alloys and hydrogen transmission pipelines. The finite element method has become an essential tool for investigating hydrogen diffusion and the mechanisms of hydrogen embrittlement; numerical simulations can reveal the diffusion behaviour of hydrogen in metals, stress-strain interactions, and their effects on microstructure and mechanical properties. In this paper, ABAQUS software is employed to simulate and analyse the hydrogen concentration distribution in 80S steel under different hydrogen charging conditions, based on hydrogen diffusion theory and mechanical models, with the aim of investigating the mechanism of hydrogen permeation and providing a reference for the design of high-strength steel to resist hydrogen embrittlement.

Keywords: 80S Steel; Finite Element Analysis; Mechanical Properties.

1. Introduction

Once hydrogen penetrates the interior of a metal, it can cause a significant reduction in the material's ductility and toughness, and may even lead to brittle fracture; since such brittle fracture occurs without any obvious warning signs, this phenomenon is known as hydrogen embrittlement. In the case of high-strength 80S steel,[1-2] which is widely used in hydrogen storage facilities, sensitivity to hydrogen embrittlement increases with rising strength, making the risk of hydrogen-induced failure particularly pronounced. Consequently, a systematic investigation into the permeation behaviour of hydrogen in 80S steel pipes and the quantitative patterns of its influence on mechanical properties holds significant theoretical and engineering value for assessing the safety of pipe columns and formulating scientifically sound protective strategies.

As hydrogen flows through the pipe, hydrogen atoms cause a deterioration in the mechanical properties of the metal pipe during its service life. Zhang Shukun et al.[3] investigated the hydrogen diffusion characteristics in X80 steel welded joints and their relationship with temperature through detailed simulation analyses.Chen Kai et al.[4] used finite element analysis to investigate the hydrogen permeation behaviour of X80 pipeline steel of varying thicknesses under electrochemical hydrogen charging conditions, as well as the effect of pre-charging time on the material's mechanical properties. Zheng Shi[5] investigated hydrogen permeation behaviour under various conditions and the effect of hydrogen on the mechanical properties of the material, and fitted the patterns of influence of different hydrogen concentrations on these mechanical properties. Taolong Xu et al.[6] analysed the hydrogen diffusion process under the combined influence of residual stress fields and hydrogen concentration fields, taking into account the effects of structural inhomogeneities in the weld zone.

2. Numerical Simulation of Hydrogen Permeation and Tensile Behaviour in 80S Steel under Different Hydrogenation Conditions

In finite element simulations, the diffusion of hydrogen atoms obeys the law of conservation of mass and is driven by a chemical potential gradient. The driving force for diffusion can be expressed as a gradient of the chemical potential (μ); this is typically converted into a concentration-driven term using a mass flux formulation. Specifically, the diffusion of hydrogen atoms in steel can be described by the following mass conservation equation:

$$\frac{\partial C}{\partial t} + \nabla \cdot J = 0 \tag{1}$$

Here, C represents the hydrogen concentration (units: mol/m³), t represents time (units: s), and J represents the hydrogen diffusion flux (units: mol/(m²·s)). According to the theory of irreversible thermodynamics, the diffusion flux can be expressed as a linear function of the chemical potential gradient:

$$J = -M \cdot \nabla \mu \tag{2}$$

In the equation, M represents the mobility of hydrogen atoms (unit: mol²·s/(kg·m³)), and μ represents the chemical potential (unit: J/mol). For the problem of hydrogen diffusion in steel, the chemical potential can be expressed as the sum of the concentration term and the stress term:

$$\mu = \mu_0 + RTln(\theta) - \sigma_h V^{-}_{H} \tag{3}$$

Here, μ_0 is the standard chemical potential (unit: J/mol), R is the gas constant (8.314 J/(mol·K)), T is the absolute temperature (unit: K), θ is the hydrogen occupancy (defined as the ratio of hydrogen concentration to interstitial site density, i.e. θ = C/NL, where NL is the interstitial site density), σ_h is the hydrostatic stress (unit: Pa), V_H is the partial molar volume of hydrogen (unit: m³/mol).

Substituting the chemical potential expression into the flux equation and expanding it using the chain rule yields an explicit expression for the diffusion flux:

$$J = -D \cdot \nabla C + \frac{DCV_H}{RT} \nabla \sigma_h \tag{4}$$

Here, D = M·RT/C represents the diffusion coefficient of hydrogen (unit: m^2/s); this coefficient is independent of concentration and depends solely on temperature. The above equation clearly reveals that the hydrogen diffusion flux consists of two terms: the first is the Fickian diffusion term driven by the concentration gradient, and the second is the stress-assisted diffusion term driven by the stress gradient. The stress gradient term reflects the 'trapping' effect of the hydrostatic tensile stress zone on hydrogen atoms and is the key physical mechanism for explaining the hydrogen-induced cracking mechanism.

Substituting the flux expression into the mass conservation equation yields the governing differential equation for hydrogen diffusion:

$$\frac{\partial C}{\partial t} = \nabla \cdot (D \nabla C - \frac{DCV_H}{RT} \nabla \sigma_h) \tag{5}$$

This equation constitutes a hydrogen diffusion model that accounts for stress-diffusion coupling effects, commonly referred to as the 'stress-assisted diffusion equation'. In finite element implementations, this equation can be solved using either sequential coupling or fully coupled methods: first, the stress field is calculated via mechanical analysis, and the hydrostatic stress gradient is extracted; subsequently, the stress field is introduced as a predefined field into the mass diffusion analysis step to solve for the spatio-temporal evolution of the hydrogen concentration field. It is worth noting that the variation of the hydrostatic stress field with the distribution of hydrogen concentration is a dynamic coupling process; for strongly coupled problems, an iterative solution strategy must be employed.

To solve the equation numerically, appropriate initial and boundary conditions must be defined. The initial condition is typically set as the initial hydrogen concentration distribution C(x,0) = C0. Boundary conditions can be divided into two categories: the first type (Dirichlet boundary conditions) specifies the hydrogen concentration values at the boundary, used to simulate contact with a hydrogen-containing environment; the second type (Neumann boundary conditions) specifies the hydrogen flux at the boundary, such as a no-flux boundary J·n = 0, or a boundary with a specified permeation flux.

By establishing the finite element framework described above, it is possible to quantitatively predict the spatiotemporal distribution of hydrogen within steel components, assess the risk of hydrogen embrittlement under complex stress conditions, and provide a theoretical basis for hydrogen embrittlement-resistant design and service life assessment.

The model employs eight-node thermally coupled hexahedral elements (HC8P) to solve the hydrogen diffusion problem. These elements support the simulation of heat conduction-diffusion equations, modelling the hydrogen diffusion process via an equivalent heat conduction mechanism, thereby achieving coupling between the mechanical and diffusion fields. Regarding material parameters, physical parameters such as the hydrogen solubility and diffusion coefficient of 80S steel were input, along with mechanical parameters including the elastic modulus and hardening law. The boundary conditions include:[7] (1) a constant hydrogen concentration applied to the outer surface of the tube (corresponding to different electrochemical hydrogenation current densities); (2) zero-flux boundaries at the internal surface and the axial plane of symmetry; (3) an axial displacement boundary is introduced during tensile loading, ensuring that the steel tube is subjected to axial tensile stress during the simulation. This simulation framework enables the calculation of hydrogen concentration fields under various operating conditions and the analysis of the results.

ABAQUS simulations were performed to investigate the hydrogen concentration distribution in 80S steel under different pre-hydrogenation times.[8] The model utilised eight-node heat-conducting hexahedral elements, with hydrogen atom diffusion governed by the principle of mass conservation. Assuming that diffusion is driven by chemical potential, the driving force is given by:

$$J = -\mathrm{s}D\left\{\frac{\partial \Phi}{\partial x} + \kappa_p \frac{\partial p}{\partial x}\right\} \tag{6}$$

In the equation, s represents the solubility of hydrogen, in $cm \cdot MPa^{-0.5}$; D represents the diffusion coefficient, in $cm^2 \cdot s^{-1}$; Φ represents the hydrogen activity, in $MPa0.5 \cdot cm^{-1}$; κp represents the stress coefficient at equivalent pressure; and p represents the hydrostatic stress, in MPa.

Based on LAMMPS molecular dynamics simulations, the tensile deformation of hydrogen-containing metal columns was modelled to determine the trends in microstructural proportions at different hydrogen concentrations. The simulations were based on the following assumptions: (1) the microstructure of the specimen is homogeneous; (2) the temperature remains constant throughout the process; (3) the hydrogen concentration on the surface is uniformly distributed and constant.

3. Analysis of the Effects of Hydrogen Permeation in 80S Steel

In order to visually demonstrate the effect of hydrogen on the mechanical properties of the pipe material under different hydrogen-charging conditions, it is necessary to use corresponding hydrogen concentration distributions to illustrate the variation in hydrogen concentration gradients under these conditions. Figure 1 shows cross-sectional diagrams of the hydrogen concentration gradient at the surface and centre of an 80S pipe specimen following electrochemical hydrogenation. The distribution pattern in the figure reveals that the hydrogen concentration peaks at the specimen's edges and decreases gradually from the edges towards the centre, with the hydrogen concentration at the specimen's centre being the lowest within the entire observation area. When the current density was 50 $mA \cdot cm^{-2}$, the hydrogen concentration at the specimen edge was 3.650×10^{-4} $mol \cdot cm^{-3}$. As the hydrogen charging current density increased, the number of hydrogen atoms penetrating into the interior of the specimen increased, and the hydrogen concentration in both the edge and central regions of the specimen gradually rose. Compared with the specimen subjected to a hydrogen-charging current density of 10 $mA \cdot cm^{-2}$, the hydrogen concentration at the edge of the specimen subjected to a current density of 50 $mA \cdot cm^{-2}$ increased by a factor of 3.279.

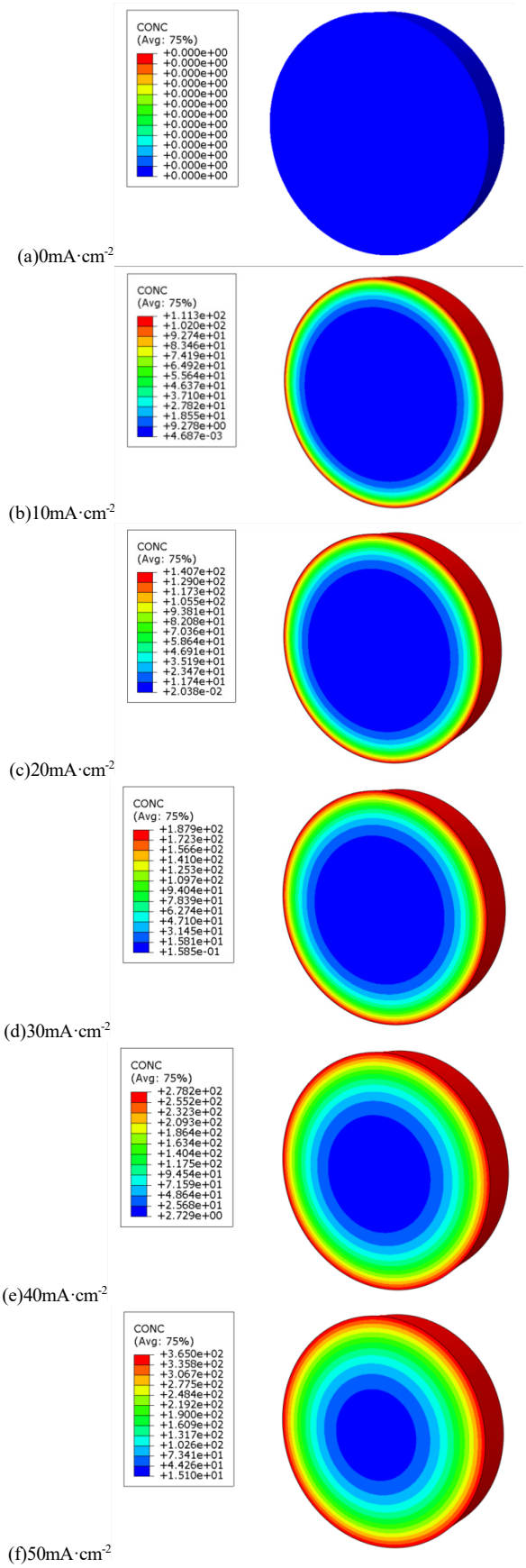


Fig 1. Hydrogen concentration distribution in 80S steel at different hydrogen charging current densities

This set of images illustrates the spatial distribution characteristics of hydrogen concentration (CONC) in 80S steel under different current density conditions (0–50 mA·cm⁻²), reflecting the diffusion and enrichment behaviour of hydrogen within the material during the electrochemical hydrogenation process.

Overall, as the current density gradually increases, the hydrogen concentration rises significantly and the concentration gradient gradually strengthens. Under the (a) 0 mA·cm⁻² condition, the interior of the specimen exhibits a uniform low-concentration state with virtually no hydrogen penetration, indicating that hydrogen diffusion within the material is negligible when no current is applied, remaining at an initial or background level.

When the current density was increased to 10 mA·cm⁻² (Figure b), a distinct hydrogen enrichment phenomenon began to appear on the surface of the material, forming a concentration gradient that decreased from the exterior towards the interior. At this point, hydrogen was primarily concentrated near the surface, whilst the interior maintained a relatively low concentration, indicating that hydrogen diffusion was still in its early stages and that the diffusion depth was limited[9].

Upon further increasing the current density to 20 mA·cm⁻² and 30 mA·cm⁻² (Figures c and d), a marked rise in hydrogen concentration can be observed, with the high-concentration region gradually expanding inwards and the concentration contour lines becoming denser. This indicates that the driving force for diffusion has increased, leading to a higher rate of hydrogen migration within the material. Concurrently, the concentration gradient becomes steeper, suggesting that the diffusion process is driven more significantly by the concentration gradient.

Under conditions of 40 mA·cm⁻² and 50 mA·cm⁻² (Figures e and f), hydrogen concentrations reached their highest levels, and the high-concentration zones had clearly penetrated into the interior of the specimen, with extensive high-concentration regions even appearing. This indicates that, at high current densities, the rate of hydrogen generation increases significantly, leading to a rapid accumulation of hydrogen at the surface and the formation of a strong diffusion driving force, which causes hydrogen to penetrate rapidly into the interior. At the same time, the concentration gradient between the surface layer and the interior further increases, potentially triggering stronger hydrogen-induced stresses and a higher risk of damage.

In terms of distribution patterns, all figures exhibit a typical radial distribution characterised by higher concentrations at the outer regions and lower concentrations at the centre, consistent with Fick's law of diffusion, whereby hydrogen migrates from regions of high concentration (the surface) to regions of low concentration (the interior). Furthermore, as the current density increases, the concentration contour lines gradually become denser, reflecting an increase in the concentration gradient and a corresponding enhancement in the diffusion flux.

In summary, the finite element results from this study indicate that current density is a key parameter governing hydrogen permeation behaviour. Higher current densities result in higher hydrogen concentrations within the material, greater diffusion depths and steeper concentration gradients, thereby significantly increasing the potential risk of hydrogen embrittlement and hydrogen damage in the material[10]. This principle provides important guidance for the safety assessment of hydrogen storage tubing during service and for the design of hydrogen-damage-resistant structures.

4. Conclusion

This paper systematically investigates the hydrogen

permeation behaviour in 80S steel under electrochemical hydrogen charging conditions using the finite element method. The results indicate that current density significantly influences the distribution of hydrogen concentration and the depth of diffusion. As current density increases, hydrogen accumulates more extensively at the material's surface and continues to diffuse into the interior, forming a pronounced concentration gradient, thereby increasing the risk of hydrogen-induced damage. These findings provide a theoretical basis for assessing the in-service safety of hydrogen storage tubing materials and for designing them to resist hydrogen embrittlement.

References

[1] Yao Chan, Chen Jian, Ming Hongliang, et al. Research progress on hydrogen permeability behavior of pipeline steel[J]. Journal of Chinese Society for Corrosion and Protection, 2023,43(02):209-219.

[2] Zhu Shidong, An Haijuan, Mao Keyan, et al. Research progress on hydrogen embrittlement susceptibility of high-pressure pipeline steel welded joints[J]. Corrosion & Protection, 2025,46(12):1-13.

[3] Zhang Shukun, Wang Zhikun, Lv Jjiahua, et al. Numerical simulation study on hydrogen diffusion mechanism at welding joints and defects in hydrogen pipeline[J]. Nonferrous Metals, 2025,15(02):225-230.

[4] Chen Kai, Du Yifan, Xu Haoyun, et al. Hydrogen permeation and hydrogen embrittlement sensitivity of X80 pipeline steel[J]. Journal of Chinese Society for Corrosion and Protection, 2025,45(02):388-396.

[5] Zheng Shi. Study on hydrogen permeation and hydrogen-induced mechanical property degradation behavior in X80 pipeline steel[D]. University of Science and Technology Beijing, 2025.

[6] Xu T ,Guo S ,Fu B , et al.Hydrogen diffusion simulation of the X80 pipeline steel girth weld zone considering the synergistic effect of the structure–stress–concentration field[J]. Engineering Failure Analysis, 2024,160108205.

[7] Guo Shiwei, Wu Haozhi, Dong Shaohua, et al. Simulation of hydrogen distribution in pipeline with double corrosion defects[J]. Journal of Chinese Society for Corrosion and Protection, 2024,44(02):335-344.

[8] Zhang Timing, Zhao Weimin, Jiang Wei, et al. Numerical simulation of hydrogen diffusion in X80 welded joint under the combined effect of residual stress and microstructure inhomogeneity[J]. Acta Metallurgica Sinica, 2019,55(02):258-266.

[9] Kumar M M , Kumar M G ,Singh P A , et al.Enhanced resistance to electrochemical degradation and hydrogen permeation by grain boundary and strain engineering in cobalt-graphene oxide composite coatings[J]. Materials Characterization, 2024,217114377-114377.

[10] Gao Jin, Li Ba, Song Weicheng, et al. Discussion on hydrogen embrittlement sensitivity of girth weld of L245 pipeline steel under 4 MPa hydrogen environment[J]. Metallurgical Analysis, 2023,43(09):86-94.